This is an Accepted Manuscript of an article published by Taylor & Francis in International Journal of Sustainable Transportation on 11 Feb 2021 (published online), available at: http://www.tandfonline.com/10.1080/15568318.2020.1871129

# Tidal phenomenon of the dockless bike-sharing system and its causes: the case of Beijing

Xiaoyue Tan[a,b], Xiaolin Zhu[b], Qiang Li[a,*], Luning Li[a], Jin Chen[a]

[a]*Faculty of Geographical Science, Beijing Normal University, Beijing, 100875, China*

[b]*Department of Land Surveying and Geo-Informatics, The Hong Kong Polytechnic University, Hong Kong, China*

*Email of corresponding author: liqiang@bnu.edu.cn

# Tidal phenomenon of the dockless bike-sharing system and its causes: the case of Beijing

**Abstract:** Dockless bike-sharing system, as a flexible and eco-friendly solution to improve urban public transportation, has rapidly expanded in many cities around the world. The higher flexibility of the dockless bike-sharing system produces more significant tidal phenomenon that leads to serious traffic problems. However, as a new travel mode, the spatiotemporal characteristics of tidal phenomenon of the dockless bike-sharing system is unknown. This study proposed a method to quantify tidal traffic patterns of shared bikes in Beijing, the capital and megacity of China, and then applied multinomial logit model to reveal main causes of these patterns. Five traffic patterns were found on weekdays, among which three patterns display extreme convergence and divergence states during morning and evening rush hours. Only three patterns exist on weekends and the tidal traffic phenomenon becomes less intensive but lasts longer. Population is the most decisive factor, which determines the density of total traffic flow. Subsequently, resident-employment ratio controls the direction of commute flows thus causing tidal traffic on weekdays, while land use diversity and factors related to leisure activities are more influential on weekends. With the knowledge of tidal phenomenon of dockless bike-sharing usage, some operational strategies were suggested, such as optimizing the stock of the shared bikes in different time and locations, which will benefit bike-sharing enterprises and the local administrators to mitigate problems caused by tidal traffic and promote the usage and efficiency of dockless bike-sharing system.

**Keywords:** dockless bike-sharing system; tidal traffic phenomenon; convergence and divergence; human mobility; transit-oriented development (TOD); Beijing

## 1. Introduction

To achieve the goal of sustainable development, transit-oriented development (TOD) has become the focus of urban planning and management around the world (Cervero et al., 2002; Duncan, 2011; Nasri & Zhang, 2014), thanks to its advantages in improving land use efficiency, reducing traffic congestion and greenhouse gas emissions. The core of TOD is to make full use of the public transportation system, focusing on improving accessibility to public transportation system. The emerging bike-sharing (also called bicycle-sharing) system provides a low-cost and flexible mobility option to supplement public transportation system, especially for short distance trips (Jäppinen et al., 2013). It plays an important role in TOD and thus has attracted increasing attention during the past decade.

Currently, the bike-sharing system has been spreading around the world, which can be generally grouped into two types with and without dock stations (Figure 1). The first type became popular since 2005 (DeMaio, 2009) and has been adopted in more than 850 cities over the world (Fishman, 2016a), which only allows users to pick up and return a bike at fixed dock stations that set up in advance. The second type, known as dockless bike-sharing system has been flourishing since 2015 in China, Singapore, UK and USA along with the development of GPS-enabled phones, mobile payment and Internet of Things (IoT) (Shen et al., 2018). More than 19 million dockless shared bikes have been deployed in about 360 cities in China by 2019 (Chen, 2019). The system uses a smartphone App to locate and unlock bikes, and charging an hourly rate for use, allowing users to pick and return a bike at any places. Accordingly, the dockless bike-sharing system not only brings great convenience and flexibility for selecting start and end point of a short distance trip, but also saves the capital and urban land for the construction of dock stations. On the other hand, it also produces many problems such as indiscriminate parking, deterioration of urban landscape, obstruction of normal vehicle and pedestrian traffic, low bike utilization efficiency of over-supply and so on (Zhang et al., 2019). Such problems are further aggravated during a certain period of a day (e.g. commuting time) and in specific areas (e.g. metro or subway stations) due to function types of neighborhood and commuting behaviour of users. For instance, a large number of bikes are piled up in some metro or subway stations close to the residential area during the morning commuting peak due to large arrival flow, while it is difficult to find an available bike in the same stations during the afternoon commuting peak because of greater departure flow. Such phenomenon occurs periodically and presents a fixed temporal pattern, and thus is called the tidal phenomenon of a bike-sharing system (Fishman, 2016b). Obviously, the higher flexibility of the dockless bike-sharing system makes the tidal phenomenon more significant than that of dock-based system, resulting in more serious traffic problems. In order to alleviate adverse impacts of the dockless bike-sharing system, it is necessary to quantify the spatially explicit tidal phenomenon, which will benefit bike-sharing enterprises and the local administrators to implement effective operation and management strategies, such as optimizing the supply of the shared bikes in different time and locations and so on.

[Figure 1 near here]

However, the spatiotemporal pattern of tidal phenomenon of dockless bike sharing system is not explicitly clear. Since traditional docked bike-sharing system does not present significant tidal phenomenon due to the limited and fixed number of dock stations, existing studies targeting the traditional docked bike-sharing system mainly focused on the spatiotemporal patterns of the usage of bike sharing system in city-level or station-level (Borgnat et al., 2011; Faghih-Imani & Eluru, 2016; Zaltz

Austwick et al., 2013), travel behaviour of shared-bike users (Faghih-Imani & Eluru, 2015; Fishman et al., 2014), and determinants of bike-sharing trips (El-Assi et al., 2017; Faghih-Imani et al., 2014; Faghih-Imani & Eluru, 2016; Zhang et al., 2017). On the other hand, as the dockless bike-sharing system based on mobile phones and mobile payment emerged in recent years, only a few studies conducted quantitative analysis of dockless bike-sharing data but did not explored the tidal phenomenon. For example, Shen et al. (2018) examined the spatiotemporal distributions of the dockless bike-sharing usage as well as the impact of weather conditions on it. Xu et al. (2019) revealed the temporal usage pattern of dockless bike-sharing at different places using four-month bike-sharing trip data in Singapore, and identified some built environment indicators that are correlated with these patterns. He et al. (2018) identified the spatial clusters of dockless bike-sharing trips by searching for the strongest spatial linkage for each bike-sharing trip within a certain distance, and found that most of the clustering results presented a strong spatial linkage with metro stations in a China's megacity, Shenzhen. Fortunately, with the emergence of new big data sources (e.g., social media and mobile phone data) that can reflect human spatiotemporal behavioural regularity, recent studies have proposed indicators and methods to characterize the aggregation and dispersion patterns of human beings. For instance, Liu et al. (2012) linked urban land use to traffic source and sink areas using the taxi trajectory dataset in Shanghai. The source area was referred to having more taxi pick-up than drop-off, and sink area as having more taxi drop-off than pick-up. Yang et al. (2016) further defined human convergence as that the number of flowing to a location is larger than the number of outgoing people, and human divergence as the opposite situation that the number of leaving people is larger. And then human spatial convergence and divergences in Shenzhen were subsequently explored using mobile phone dataset. Since tidal phenomenon of shared bikes are similar to the convergence and divergence (or source and sink) of people, these definitions and methods could be adopted to study tidal phenomenon of dockless bike-sharing system.

Considering the importance of the tidal phenomenon for the dockless bike-sharing system, the study firstly proposed a method to quantify it by defining the convergence and divergence state of shared bikes and further deriving tidal traffic patterns. Moreover, we explored the causes of the tidal traffic phenomenon by the Multinomial Logit Model (MNLM). We selected Beijing city as a case study and collected the dockless bike-sharing trip dataset in the city during $10^{th}$ to $16^{th}$ May 2017. The paper is organized as follows. Section 2 introduces study area and data. Section 3 describes the analytical framework for quantifying tidal phenomenon. Section 4 and Section 5 present the tidal traffic patterns and discuss the role of various influential factors. The final section gives the conclusions.

## 2. Study area and dataset

As the capital of China and one of the world-class megacities, Beijing has more than 20 million permanent population and a developed public metro network with more than 20 lines and 300 stations up to 2018 (Beijing Subway, 2018). With the promotion of TOD, the dockless bike-sharing system has been widely used in recent years, playing an increasingly significant role in public transport. The bike-sharing dataset was collected from the Beijing Mobike Technology Co., Ltd, one of the largest dockless bike-sharing system operators in China. The dataset contains more than 3 million bike-sharing trips from May 10 (Wednesday) to May 16 (Tuesday) 2017, a period in a favourable season for cycling. The dataset includes the location coordinates of trip origin and destination, the unlocking and locking time, user ID and bike ID. Considering that the metro stations are usually regarded as the pivots of TOD in Beijing (Lyu et al., 2016; Ma et al., 2017; Zhao & Li, 2018), only trips around 284 metro stations that opened before May 2017 (the origin or destination of trips within a buffer zone defined in section 3.1) were extracted for the following analysis (Figure 2), which dominates the trips of bike-sharing system in Beijing.

[Figure 2 near here]

Moreover, we also collected demographic and point of interest (POI) data in 2018 (Figure 3), which provide information of possible factors influencing the tidal phenomenon. The demographic data is gridded data with spatial resolution of 300m, recording number of people working and residing in each grid, provided by China Academy of Urban Planning & Design. POI data presents the geographical location of urban facilities and land use functions, obtained from AutoNavi (www.amap.com), one of the largest Internet map service providers in China. Certain categories of POIs, namely resident places, catering services, life services and shops, entertainment and sports venue, medical services and hospitals, science/education institutions, tourist attractions and companies, were counted and plotted to roughly illustrate the distribution of human activities inside the 6th Ring Road in Beijing (Figure 3.c).

[Figure 3 near here]

## 3. Methodology

### *3.1 Definition of tidal traffic patterns*

The tidal phenomenon can be characterized by tidal traffic patterns, i.e., various combinations of convergence and divergence state of shared bikes, so we firstly defined convergence and divergence state respectively referring to previous research on human convergence (Yang et al., 2016). Since the origin and destination of each bike-sharing trip were recorded in the data used in this study, in a designated area, the arrival flow can be defined as the cumulative arrival trips, whereas the departure flow can be defined as the cumulative departure trips. Consequently, during a certain time period *t*, the net flow in a designated area can be defined as follows:

$$netflow_t = arrival\ flow_t - departure\ flow_t \tag{1}$$

A positive net flow indicates more bikes arriving to the area, defined as convergence state (Figure 4.a). Conversely, a negative net flow indicates more bikes departing from the area, defined as divergence state (Figure 4.b). It is obvious that if the convergence exceeds a certain threshold, a large number of shared bikes will pile up in the designated area. On the other hand, the divergence may alleviate the mentioned problems, but a continuous and strong divergence easily leads to a short supply of shared bikes that influences usage efficiency and user's satisfaction.

[Figure 4 near here]

To identify the tidal traffic patterns along with time, the arrival flow and departure flow of bike-sharing trips for each metro station were calculated at intervals of one hour over one week. For all stations, we constructed the spatiotemporal matrix $A[i, t, k]$ of arrival flow and matrix $D[i, t, k]$ of departure flow in Beijing, here $i$ represents metro station index ($i = 1,\ldots, 284$) and $t$ represents hour of a day ($t = 1, \ldots, 24$) and $k$ represents day of a week ($k = 1, \ldots, 7$). Considering the great difference of bike-sharing trips on weekdays and weekends (Faghih-Imani & Eluru, 2015), the spatiotemporal matrixes were decoupled into weekdays and weekends and further averaged according to Eqs. (2)-(5).

$$\bar{A}_{weekday}[i,t] = \text{Ave}\ (A[i,\mathrm{t},\mathrm{k}]), k = 1,2,3,4,5 \tag{2}$$

$$\bar{D}_{weekday}[i,t] = \text{Ave}\ (D[i,\mathrm{t},\mathrm{k}]), k = 1,2,3,4,5 \tag{3}$$

$$\bar{A}_{weekend}[i,t] = \text{Ave}\ (A[i,\mathrm{t},\mathrm{k}]), k = 6,7 \tag{4}$$

$$\bar{D}_{weekend}[i,t] = \text{Ave}\ (D[i,\mathrm{t},\mathrm{k}]), k = 6,7 \tag{5}$$

Based on Eq. (1), the convergence-divergence matrix (*CDM*) can be calculated following Eqs. (6)-(7):

$$CDM_{weekday}[i,t] = \bar{A}_{weekday}[i,t] - \bar{D}_{weekday}[i,t] \tag{6}$$

$$CDM_{weekend}[i,t] = \bar{A}_{weekend}[i,t] - \bar{D}_{weekend}[i,t] \tag{7}$$

Figure 4.c illustrates *CDM* variation and corresponding tidal traffic patterns. At time $t$ and station $i$, the positive element value of *CDM* represents a convergence state of shared bikes, while the negative element value of *CDM* represents a divergence state of shared bikes, and the element value of *CDM* approximating zero suggests dynamic equilibrium for the arrival flow and departure flow.

Besides the net flow, the total flow (*TF*) that is the sum of arrival flow and departure flow of shared bikes is also essential to reflect the intensity of bike-sharing trips around a metro station. Similarly, *TF* on weekdays and weekends were calculated respectively at each hour $t$ and each metro station $i$ by using Eq. (8)-(9).

$$TF_{weekday}[i,t] = \overline{A}_{weekday}[i,t] + \overline{D}_{weekday}[i,t] \tag{8}$$

$$TF_{weekend}[i,t] = \overline{A}_{weekend}[i,t] + \overline{D}_{weekend}[i,t] \tag{9}$$

For calculating arrival flow, departure flow and net flow, the size of the designated area needs to be defined. As shown in Figure 5, the size of a designated area for each station is outlined as a buffer zone around a metro station with radius *r* that covers all exits of the metro station and is within an acceptable walking distance for finding available bikes (blue area in Figure 5, named station cell). Since the speed of a normal walker is generally 60-80m/min, 300m is considered as an appropriate walking distance for finding an available bike (Zhang et al., 2017), so that the radius *r* was set to 300m around a station.

[Figure 5 near here]

### *3.2 Cluster analysis*

Based on *CDM* and *TF* on weekdays and weekends, K-means cluster method (Dangeti, 2017) was employed to classify all stations into several groups. The elbow method and prior knowledge about traffic flow were combined to determine the optimal number of clusters (*k*). First, calculate the within-cluster-sum of squared Errors (*SSE*) for each value of *k*, and then the optimal *k* should be the one for which *SSE* stops sharp falls, i.e., adding another cluster does not distinctly decrease *SSE*. However, the elbow method sometimes gives ambiguous *SSE* dropping trend. Thus, in practice, we first determine a reasonable range of *k* based on the elbow method, and then draw all the clustering results to ascertain the optimal *k* according to prior knowledge on human mobility in cities. The specific convergence and divergence patterns for each group were further analyzed in the results section.

### *3.3 Deriving the influential factors*

To figure out causes of tidal traffic patterns, several possible factors in term of demographic attribution, traffic conditions and land use were considered according to the previous studies (Etienne & Latifa, 2014; Faghih-Imani et al., 2014; Gu et al., 2019; Nasri & Zhang, 2014; Shen et al., 2018; Vogel et al., 2011; Yang et al., 2019; Zhang et al., 2018, 2017). To derive these factors, the bike-sharing coverage area was firstly defined and all the influential factors were calculated within the coverage area. Here the bike-sharing coverage area is defined as a larger buffer zone with radius $R$ covering most possible trips from/to the station (orange area in Figure 5). Since riding distance of over 80% bike-sharing trips in Beijing are within 1000m according to our trip data, the radius $R$ of bike-sharing coverage area was set to 1000m, which not only covers most of the shared bicycle trips at each station, but also ensures that the overlap area between any two stations is minimal.

Four factors were selected to indicate demographic attribute, i.e., population density, resident density, employment density and resident-employment ratio. Resident density and employment density in each bike-sharing coverage area were calculated from population dataset recording number of people residing and working in the grid. Population density is the sum of resident density and employment density in each bike-sharing coverage area, while the resident-employment ratio is resident density divided by employment density. Meanwhile, four factors related to traffic conditions are: length of roads (excluding highways and viaducts), representing basic cycling infrastructure; intersection density, representing network connectivity; density of bus stops and number of exits of a metro station, both representing public transport accessibility.

A total of 13 factors were calculated using the POI data to reflect the influences of land use, include land use diversity, land use density, and density of urban facilities with 11 specific functions (restaurants, pubs/bars, theaters, shops, parks, universities and others in Table 1). Land use diversity ($LU_d$) within a coverage area was calculated using Shannon's diversity index:

$$LU_d = -\sum_{k=1}^{n} P_k \ln (P_k) \tag{10}$$

where $P_k$ is the proportion of POI type $k$ in one bike-sharing coverage area, i.e., the ratio of POI type $k$ to the total number of POIs in the area. Land use density is represented by the amount of all kinds of POIs within the coverage area. To get a more representative value to reflect the size of facilities, we did not merge the details POIs within universities and parks. For example, for a university with 20 buildings marked as POIs in a bike-sharing coverage area, the land use density of this university was counted as 20 rather than 1. Table 1 lists all possible factors and descriptive statistics for 284 bike-sharing coverage areas in Beijing.

[Table 1 near here]

### *3.4 Multinomial logit model*

The Multinomial Logit Model (MNLM) was employed to quantify contributions of abovementioned factors respectively, considering that the MNLM can generalize logistic regression to multi-category problems and is often used to predict probabilities of different possible outcomes for the given dependent variables (Greene, 2003). The fundamental formula of the MNLM is described as follows, supposed that there are *K* explanatory variables $X_1$, $X_2, \ldots, X_K$ and the outcome variable is *Y* with *J* category.

$$\ln \Omega_{j|b}(\mathrm{X}) = \ln \frac{\Pr(y = j|\boldsymbol{X})}{\Pr(y = b|\boldsymbol{X})} = \beta_{j0} + \beta_{j1}X_1 + \beta_{j2}X_2 + \cdots + \beta_{j\mathrm{K}}X_K \quad \text{for } j=1, \ldots, J \tag{11}$$

where $\ln \Omega_{j|b}(\mathrm{X})$ is the log-odd of category *m* compared to base category *b*. The coefficient $\beta_{jk}$ means a logit change with one-unit increase of the explanatory variable $X_k$ under the condition of other variables unchanged. A base category $b$ is usually designated among $J$ categories so that the probabilities of other $J$-1 categories can be compared to the probability of base category $b$, thus $J$-1 logit equations were obtained. The probabilities of $J$ categories can be predicted by solving $J$ equations according to Eq. (12) with the maximum likelihood method.

$$\Pr(y = j|\mathrm{X}) = \frac{\exp(X\beta_{j|b})}{\sum_{j=1}^{J} \exp(X\beta_{j|b})} \text{ for } j = 1, \dots, J \tag{12}$$

Then Relative Risk Ratio (*RRR*), the most widely used parameter for MNLM model interpretation, can be calculated using Eq. (13):

$$RRR = \frac{\Pr(y = j|\mathrm{X})}{\Pr(y = b|\mathrm{X})} = \exp\left(\beta_{j0} + \sum_{k=1}^{K} \beta_{jk} X_K\right) \tag{13}$$

*RRR* is a ratio of two probabilities as an exponential function with regression coefficients. *RRR* larger than 1 shows a relatively larger chance that the outcome falling in $j$ category rather than base category $b$ and this relative chance grows with the increases of explanatory variable values, indicating a positive effect. Conversely, *RRR* less than 1 represents a negative effect. The variables with $RRR \approx 1$ would not be considered as vital decisive factors due to relative weak effects on the probability ratio of category $j$ to $b$. Note that the estimated parameters and *RRR* will change with the base category selected to interpret the logit model from different perspectives. In our study, all categories will be selected as base category by rotating.

Several pseudo $R$-squared indexes (range from 0 to 1) have been developed to evaluate the goodness-of-fit because the equivalent statistic to $R$-squared does not available for logistic models. Nagelkerke $R^2$ is one of the goodness-of-fit indicators that have a likelihood of 1 when the full model perfectly predicts the outcome. Apart from that, count $R^2$ gives predictive accuracy of the model, which is the number of correct predictions divided by total counts.

# 4. Results

## *4.1 Tidal traffic patterns on weekdays*

Based on the calculated *CDM* and *TF* of 284 public transit stations in Beijing, the tidal traffic patterns of dockless bike-sharing trips were identified by using K-means cluster analysis method. There are five patterns for weekdays and three patterns for weekends, names of these patterns and proportion of stations belonging to each pattern were listed in Table 2.

[Table 2 near here]

To intuitively visualize tidal traffic patterns of dockless bike-sharing trips in different stations, the hourly profiles of *CDM* and *TF* for different patterns were plotted and the corresponding stations belonging to each pattern were highlighted in the map (Figure 6). Both N-N-HF (Figure 6.a) and N-N-LF patterns (Figure 6.b) have no significant convergence and divergence states, indicating the arrival and departure flow of bike-sharing trips are in dynamic equilibrium. Accordingly, these two patterns can be considered as non-tidal patterns. Stations with C-D-HF pattern (Figure 6.c) witness dramatic convergence of shared bikes in the morning rush hours and considerable divergence in evening rush hours both with high total flows, while the D-C-HF pattern (Figure 6.d) is just opposite to C-D-HF pattern in terms of convergence and divergence in the morning and evening peaks. Unlike the above two patterns, CD-CD-HF (Figure 6.e) has a more complicated pattern with convergence followed by divergence in both morning and evening rash hours.

[Figure 6 near here]

As illustrated in Figure 6 and compared with Figure 3, the N-N-HF stations are mainly distributed in the centre of Beijing, where a large number of jobs, residential buildings and public services are concentrated, which may result in frequent bike sharing trips during the daytime. N-N-LF stations are mostly distributed in the suburbs with low population density, while partly located in the less populated regions of old downtown where scenic spots and administrative agencies are concentrated. C-D-HF stations are mainly located around large residential communities outside the city centre. In contrast, the D-C-HF stations are closer to the city centre and the high-tech industry/business parks. The number of CD-CD-HF stations is relatively small, and they are scattered in the mixed areas with both mature residential and commercial facilities.

### *4.2 Tidal traffic patterns on weekends*

Figure 7 shows the hourly profile of *CDM* and *TF* of the three patterns on weekends as well as the corresponding stations. It can be found that more stations were grouped into N-N-HF and N-N-LF patterns than that of weekdays. The C-D-HF pattern still exists at some stations, but its convergence and divergence are less intensive and last for longer time than that on weekdays, i.e., the convergence remains from morning peak hours to the afternoon, while the divergence lasts from 19:00 until midnight. It is obvious that the tidal phenomenon is attenuated during the weekends because of reduced commuting flows.

[Figure 7 near here]

The spatial distributions of the three patterns on weekends are similar to that in weekdays. N-N-LF stations are mainly located in the areas with less population density, while the N-N-HF stations are correspondingly distributed in the centre of Beijing. C-D-HF pattern only happens in large residential communities.

### *4.3 Influential factors of tidal traffic patterns on weekdays*

The MNLM was employed to identify the key factors and their contributions to the formation of different tidal traffic patterns. The results of the MNLM for weekdays are shown in Table 3. Nagelkerke's $R^2$ and count $R^2$ are 0.67 and 0.66 respectively, suggesting that the model gives a good explanation and a high predictive accuracy. As stated in section 2.3, a base category should be designated in the MNLM and interpretation of the model is based on the comparisons of the other categories with the base category. Accordingly, the N-N-HF pattern was selected as the first base category of the MNLM because it is the most common patterns, and the other patterns were successively taken as the base category in turn. Table 3 lists the estimated results of effective comparisons (only when the new comparison brought some unknown differences) and the influential factors with significant levels at 0.001, 0.01 and 0.05 for different base categories.

[Table 3 near here]

According to the results in Table 3, N-N-LF pattern is significantly negative correlated to population density while not significantly different with N-N-HF pattern in resident-employment ratio, indicating the low population density is a vital decisive factor of N-N-LF pattern. In addition, the probability of N-N-LF relative to N-N-HF pattern would decrease with the number of metro station exits if other variables remain unchanged, which implies that the metro system has a positive effect on promoting bike-sharing trips on weekday. Note that some variables (such as restaurant density and land use density) are significantly related to N-N-LF, but their influences are very limited since the *RRR* is approximately equal to 1.

For C-D-HF pattern compared to N-N-HF pattern, it has a significant positive correlation with resident-employment ratio. It is plausible that the numerous residents ride shared bikes going or leaving metro stations for commuting, causing the convergence and divergence of bike-sharing trips in morning and evening peaks respectively. For D-C-HF pattern compared to N-N-HF pattern, it has significant negative correlation with resident-employment ratio, showing that much more job opportunities are provided in the bike-sharing coverage area than housings, prompting more people riding from metro stations to workplaces in morning peak and further causing the divergence of bike-sharing trips. In addition, land use density and restaurant density have rather limited positive effect on D-C-HF, while university density shows a negative one. If C-D-HF pattern replaces N-N-HF as the base category, the *RRR* of resident-employment ratio decreased, indicating a stronger negative effect on D-C-HF pattern. In addition, an increase in university density would decrease the probability of pattern D-C-HF relative to C-D-HF.

Since CD-CD-HF pattern is the most complicated one among five tidal traffic patterns, the influential factors were comprehensively analyzed in the case of taking different patterns as the base category of MNLM. Population density has a positive effect on CD-CD-HF when compared with N-N-HF, but shows positive effect while set C-D-HF or D-C-HF as the base category.  It is also demonstrated that the probability of CD-CD-HF relative to C-D-HF pattern would decrease with the resident-employment ratio if other variables stay unchanged, suggesting if plenty of citizens move to and live around metro stations with CD-CD-HF pattern, then tidal traffic patterns around the station may convert to C-D-HF.

### *4.4 Influential factors of tidal traffic patterns on weekends*

The significant results of MNLM for weekends are shown in Table 4. Nagelkerke's $R^2$ is 0.49 and count $R^2$ is 0.66, indicating good performance of the estimated model. The base category of this model was originally set to N-N-LF, the most common pattern on weekends, and some other patterns were successively taken as the base category in turn in order to explain the model from multiple perspectives.

[Table 4 near here]

As demonstrated in Table 4, N-N-HF pattern is positively related to the resident density, metro station exits, pub/bar density and having a shopping mall nearby the station. Obviously, high resident density lays the foundation of massive bike-sharing flow, and convenient metro promotes more people ride shared bikes from or to the metro stations. Having a shopping mall means abundant concentrated shopping, leisure and entertainment functions, thus the arrivals and departures of bike-sharing are both frequent in these districts and contribute to the state of dynamic equilibrium.

As for the C-D-HF compared to N-N-LF, factors such as resident density, the number of metro station exits, having a shopping mall nearby the station have positive effect on it, while land use diversity and intersection density show a highly negative effect. Furthermore, C-D-HF pattern was analyzed in the case of taking N-N-HF pattern as the base category. Model result suggests that the resident density has a positive effect on C-D-HF pattern while land use diversity and pub/bar density are negatively correlated with it. That implies C-D-HF pattern is more likely to appear at metro stations surrounded by densely populated area with poor land use diversity.

## 5. Discussion

### *5.1 Comparison of tidal traffic on weekdays and weekends*

In this work, we ascertained the bike-sharing tidal patterns appeared on weekdays and weekends in Beijing based on the arrival and departure flow derived from one-week trip data. Five tidal traffic patterns were found around the metro stations on weekdays, namely N-N-LF, N-N-HF, C-D-HF, D-C-HF and CD-CD-HF. Three among them remained on weekends, N-N-LF, N-N-HF and C-D-HF, while D-C-HF and CD-CD-HF patterns disappeared. We further analyzed how the pattern of a station changes from weekdays to weekends. As illustration as Figure 8, all the N-N-LF stations on weekdays maintain the same pattern on weekends (Figure 8.a), while some stations belonging to other patterns on weekdays also changed to N-N-LF type on weekends (Figure 8.b-d), especially for N-N-HF and D-C-HF stations. The remarkable change from high flow stations (HF) to low flow stations (LF) suggested that the total flows were significantly reduced on weekends because of weekend downtime. With the decrease of commuting flows on weekends, the stations belonging to D-C-HF, CD-CD-HF no longer existed and converted to other patterns on weekends (Figure 8.d and e), because stations of both D-C-HF and CD-CD-HF patterns in weekdays are close to business districts providing massive employment opportunities. The abovementioned changes indicated that most non-equilibrium patterns on weekdays (e.g., C-D-HF, D-C-HF and CD-CD-HF) in Beijing were produced by commuting flows, which can be greatly mitigated on weekends. However, it should be noted that as one type of non-equilibrium pattern, C-D-HF stations still existed near large residential quarters on weekends, suggesting that other activities, such as shopping, extra-curricular schools and recreational activities, can also drive convergence or divergence. Compared with other studies performed in other cities, similar to Singapore (Shen et al., 2018), Beijing displayed distinction between weekdays and weekends driven by commuting activities, while no remarkable differences were found in Nice and Suzhou (O'Brien et al., 2014), probably due to different working-life style, travel behaviour, type of bike-sharing system (with and without docks), and amount of bike supply.

[Figure 8 near here]

### *5.2 Decisive factors of tidal traffic patterns*

The modeling results illustrated that population is the most decisive factor to differentiate high-flow patterns from the low-flow pattern. On weekdays, all the four high-flow patterns have an *RRR* greater than 1 when compared to N-N-LF (Figure 9.a), thus population density determines whether a substantial convergence or divergence can be formed. This conclusion is further confirmed by comparing population density and resident-employment ratio for five patterns (Figure 10.a and b) on weekdays. It can be found that the population density around the low-flow stations is evidently lower than high-flow stations, which is similar to research in other cities such as New York and Shenzhen (Faghih-Imani & Eluru, 2016; Zhang et al., 2017). On weekends, resident density is considered as the key factor to distinguish high- and low-flow stations according to the *RRR* (Figure 9.b), and as illustrated in Figure 10.b, N-N-LF stations are likely with less resident density.

[Figure 9 near here]

[Figure 10 near here]

For those high-flow patterns, resident-employment ratio further regulates the timing of the convergent and divergent tidal flow on weekdays, as illustrated in Figure 9.c, C-D-HF has an *RRR* of resident-employment ratio greater than 1 when compared to station with no sever tidal traffic (N-N-HF), while D-C-HF has an *RRR* of resident-employment ratio below 1. These results suggest that higher resident-employment ratio can enhance C-D-HF pattern due to commuting trips, especially in residential areas. While lower resident-employment ratio is conducive to the formation of D-C-HF patterns, especially in job quarters, and the moderate resident-employment ratio boosts CD-CD-HF accordingly (Figure 10.c).

Factors regarding land use characteristics are verified to collectively contribute to distinct the high-flow patterns, especially on weekends. According to the *RRR* values listed in Table 4, three land use variables, namely land use diversity, pub/bar density and shopping mall are crucial for the formation of tidal traffic patterns on weekends. Land use diversity represents diverse functions existing in the bike-sharing coverage area and thus affects the number of people flowing in. Shopping malls near metro stations may attract a large number of citizens to shopping and entertain on weekends. Hence, higher land use diversity, shopping malls and night spots like bars help N-N-HF stations keep high arrival and departure flows all day; stations located in less-functional districts but adjacent to a shopping mall more likely present a C-D-HF pattern. On weekdays, land use factors also contribute to separating tidal traffic patterns, such as land use diversity and density, restaurant density and university density, but their implications are slight and restricted to some specific comparisons.

As a component of public transportation system, other modes of public transportation and attributes of road network also affect the traffic flow of bike-sharing. The number of metro station exits shows a positive effect on most high-flow patterns, implying that the high convenience of metro stations promotes more people to ride shared bicycles from or to the metro stations (Figure 11.a). Density of road intersections has a negative impact on bike-sharing traffic flow on weekends but not weekdays (Figure 11.b), suggesting people are more sensitive to road conditions when traveling by bicycle on weekends.

[Figure 11 near here]

### *5.3 Mitigation of tidal phenomenon*

With the knowledge of tidal traffic patterns of dockless bike-sharing usage, associated problems could be identified and alleviated to some extent. Totally five tidal traffic patterns were found around the metro stations in Beijing. N-N-LF and N-N-HF patterns indicate dynamic equilibrium between the arrival flow and departure flow, it can be regarded as effective utilization of the sharing bicycle without problems. Consequently, only the non-equilibrium patterns (e.g., C-D-HF, D-C-HF and CD-CD-HF) should be improved, and some operational and controllable solutions should be implemented

Firstly, according to spatial distribution and temporal characteristics of the non-equilibrium stations, rebalancing strategy can be applied by adjusting the stock of bicycles in different stations or in specific periods to maintain an optimal stock distribution across the city. The rebalancing strategy was demonstrated to be effective to against tidal flows (Fishman, 2016b) . Figure 12 lists a weekly rebalancing scheme for the non-equilibrium stations, where additional management (e.g., delivery bikes from or to other places in advance, optimizing bus schedules and locations of bus stops) is required on specific days and periods of the day, taking into account the time characteristics of significant convergence and divergence states. Obviously, knowing where and when to implement additional management, as well as developing a weekly rebalancing strategy schedule, can help mitigate the problems induced by tide phenomenon.

[Figure 12 near here]

Second, fortunately there are stations with two opposite tidal traffic patterns (i.e., C-D-HF and D-C-HF) during peak hours on weekdays, accordingly shipping-in and shipping-out rebalancing strategy can be performed between these stations with opposite tidal patterns if they are adjacent to each other. Figure 13 shows the stations that can implement shipping-in and shipping-out strategy. Based on the spatial distribution of these stations, shipping-in and shipping-out stations can be optimally paired to balance the stock of bikes among these stations but with the shortest distance cost (e.g., the stations were paired within each the red dash area in Figure 13). The dynamic optimization of pairing shipping-in and shipping-out stations should be a promising solution and should be further studied in the future to mitigate problems induced by the tide phenomenon.

[Figure 13 near here]

Third, after identifying the main causes of the tide traffic patterns, in the long run, adjusting the population and its composition, traffic conditions and land use mixture is the fundamental solution to alleviate the tide phenomenon, although some of the measures are not practical in the short term due to the constraints of the fixed land use planning. At least, our study suggests that it is possible to predict the tidal traffic pattern of a station according to the demographic, traffic condition and land use characteristics within the bike-sharing coverage area. It is helpful to develop a rebalancing strategy in advance according to the tidal traffic pattern of specific stations.

## 6. Conclusions

In this work, we proposed a method to quantify the tidal phenomenon of dockless bike-sharing and further explored the possible influential factors of these tidal traffic patterns. Five patterns were found on weekends, namely N-N-LF, N-N-HF, C-D-HF, D-C-HF and CD-CD-HF, extreme convergence and divergence mainly emerge at morning and evening rash hours. Two of the patterns (D-C-HF and CD-CD-HF) do not occurred on weekends, and the tidal traffic phenomenon becomes less intensive but lasts longer. Model results show that population is the most decisive factor in Beijing, which determines the level of traffic flow on both weekdays and weekends. Resident-employment ratio further determines the direction of commute flows, thus leading to regular convergence and divergence on weekdays. Land use diversity and some specific POIs related to leisure activities (e.g., shopping malls, pub/bar) are verified to be critical influential factors on weekends, whereas most land-use-related factors are less influential on weekdays due to the heavy commuting trips. Transportation and road network conditions also involved in bike-sharing travel behaviour, better accessibility to the metro stations promotes dockless bike-sharing usage on both weekdays and weekends, while users may concern more about the road conditions on weekends and prefer biking in areas with fewer intersections. The results acquired in the study improved our knowledge of residents' travel characteristics on a kilometer-scale, and will further help us improve the first- or last-mile public transportation, which may include but not limited to bike-sharing in the future.

Although the proposed analytical framework was applicable to study the tidal phenomenon and causes of the dockless bike-sharing usage, several limitations should be further considered. First, delimiting a station cell is crucial for exploring the tidal phenomenon of bike-sharing usage, but the delimiting criteria may be adjusted according to the local urban planning, public transit conditions and people’s travel behaviour. The criteria used by our study in Beijing can be used as a reference for other cities. Second, this study focused on the spatiotemporal pattern on weekdays and weekends because the bike-sharing dataset used in this study only recorded trips within one week. However, bike-sharing trip dataset over long periods may provide new insights into tidal phenomenon of bike-sharing usage. For example, annual variations on tidal traffic may reflect changes in public transport network as well as travel behaviour over periods crossing multiple years. Last, due to the limitation of data availability, other factors such as the travel behaviour of bike-sharing users, the initial stock of shared bikes within the coverage area of each metro station, and the weather conditions were not considered in the cause analysis, which should be explored in future studies.

**Acknowledgement:**

The authors would like to thank the Academic Information Centre of Urban Planning, China Academy of Urban Planning and Design for providing part of the data. This work was supported by research grants from The Hong Kong Polytechnic University under Projects 1-ZE6Q and 9B0F, and funding from the PhD studentship of The Hong Kong Polytechnic University.

**Reference**


Borgnat, P., Abry, P., Flandrin, P., Rouquier, J.-B., & Fleury, E. (2011). Shared bicycles in a city: a signal processing and data analysis perspective. *Advs. Complex Syst*, *14*(3), 415–438. https://doi.org/10.1142/S0219525911002950

Burrough, P. A., McDonnell, R., & Lloyd, C. D. (2015). *Principles of Geographical Information Systems*. Oxford University Press.

Cervero, R., Ferrell, C., & Murphy, S. (2002). Transit-oriented development and joint development in the United States: A literature review. *TCRP Research Results Digest*, *52*.

Dangeti, P. (2017). *Statistics for machine learning*. Packt Publishing Ltd.

DeMaio, P. (2009). Bike-sharing: History, Impacts, Models of Provision, and Future. *Journal of Public Transportation*, *12*(4), 41–56. https://doi.org/10.5038/2375-0901.12.4.3

Duncan, M. (2011). The impact of transit-oriented development on housing prices in San diego, CA. *Urban Studies*, *48*(1), 101–127. https://doi.org/10.1177/0042098009359958

El-Assi, W., Salah Mahmoud, M., & Nurul Habib, K. (2017). Effects of built environment and weather on bike sharing demand: a station level analysis of commercial bike sharing in Toronto. *Transportation*, *44*(3), 589–613. https://doi.org/10.1007/s11116-015-9669-z

Etienne, C., & Latifa, O. (2014). Model-Based Count Series Clustering for Bike Sharing System Usage Mining: A Case Study with the Vélib' System of Paris. *ACM Transactions on Intelligent Systems and Technology*, *5*(3), 1–21. https://doi.org/10.1145/2560188

Faghih-Imani, A., & Eluru, N. (2015). Analysing bicycle-sharing system user destination choice preferences: Chicago's Divvy system. *Journal of Transport Geography*, *44*, 53–64. https://doi.org/10.1016/j.jtrangeo.2015.03.005

Faghih-Imani, A., & Eluru, N. (2016). Incorporating the impact of spatio-temporal interactions on bicycle sharing system demand: A case study of New York CitiBike system. *Journal of Transport Geography*, *54*, 218–227. https://doi.org/10.1016/j.jtrangeo.2016.06.008

Faghih-Imani, A., Eluru, N., El-Geneidy, A. M., Rabbat, M., & Haq, U. (2014). How land-use and urban form impact bicycle flows: evidence from the bicycle-sharing system (BIXI) in Montreal. *Journal of Transport Geography*, *41*, 306–314. https://doi.org/10.1016/j.jtrangeo.2014.01.013

Fishman, E. (2016a). Cycling as transport. *Transport Reviews*, *36*(1), 1–8. https://doi.org/10.1080/01441647.2015.1114271

Fishman, E. (2016b). Bikeshare: A Review of Recent Literature. *Transport Reviews*, *36*(1), 92–113. https://doi.org/10.1080/01441647.2015.1033036

Fishman, E., Washington, S., Haworth, N., & Mazzei, A. (2014). Barriers to bikesharing: An analysis from Melbourne and Brisbane. *Journal of Transport Geography*, *41*, 325–337. https://doi.org/10.1016/j.jtrangeo.2014.08.005

Greene, W. H. (2003). *Econometric analysis*. Pearson Education India.

Gu, Z., Zhu, Y., Zhang, Y., Zhou, W., & Chen, Y. (2019). Heuristic bike optimization algorithm to improve usage efficiency of the station-free bike sharing system in Shenzhen, China. *ISPRS International Journal of Geo-Information*, *8*(5). https://doi.org/10.3390/ijgi8050239

He, B., Zhang, Y., Chen, Y., & Gu, Z. (2018). A simple line clustering method for spatial analysis with origin-destination data and its application to bike-sharing movement data. *ISPRS International Journal of Geo-Information*, *7*(6). https://doi.org/10.3390/ijgi7060203

Jäppinen, S., Toivonen, T., & Salonen, M. (2013). Modelling the potential effect of shared bicycles on public transport travel times in Greater Helsinki: An open data approach. *Applied Geography*, *43*, 13–24. https://doi.org/10.1016/j.apgeog.2013.05.010

Liu, Y., Wang, F., Xiao, Y., & Gao, S. (2012). Urban land uses and traffic "source-sink areas": Evidence from GPS-enabled taxi data in Shanghai. *Landscape and Urban Planning*, *106*(1), 73–87. https://doi.org/10.1016/j.landurbplan.2012.02.012

Lyu, G., Bertolini, L., & Pfeffer, K. (2016). Developing a TOD typology for Beijing metro station areas. *Journal of Transport Geography*, *55*, 40–50. https://doi.org/10.1016/j.jtrangeo.2016.07.002

Ma, X., Chen, X., Li, X., Ding, C., & Wang, Y. (2017). Sustainable station-level planning: an integrated transport and land use design model for transit-oriented development. *Journal of Cleaner Production*, *170*, 1052–1063. https://doi.org/10.1016/j.jclepro.2017.09.182

Nasri, A., & Zhang, L. (2014). The analysis of transit-oriented development (TOD) in Washington, D.C. and Baltimore metropolitan areas. *Transport Policy*, *32*, 172–179. https://doi.org/10.1016/j.tranpol.2013.12.009

O'Brien, O., Cheshire, J., & Batty, M. (2014). Mining bicycle sharing data for generating insights into sustainable transport systems. *Journal of Transport Geography*, *34*, 262–273. https://doi.org/10.1016/j.jtrangeo.2013.06.007

Shen, Y., Zhang, X., & Zhao, J. (2018). Understanding the usage of dockless bike sharing in Singapore. *International Journal of Sustainable Transportation*, *12*(9), 686–700. https://doi.org/10.1080/15568318.2018.1429696

Vogel, P., Greiser, T., & Mattfeld, D. C. (2011). Understanding bike-sharing systems using Data Mining: Exploring activity patterns. *Procedia - Social and Behavioral Sciences*, *20*, 514–523. https://doi.org/10.1016/j.sbspro.2011.08.058

Xu, Y., Chen, D., Zhang, X., Tu, W., Chen, Y., Shen, Y., & Ratti, C. (2019). Unravel the landscape and pulses of cycling activities from a dockless bike-sharing system. *Computers, Environment and Urban Systems*, *75*, 184–203. https://doi.org/10.1016/j.compenvurbsys.2019.02.002

Yang, X., Fang, Z., Xu, Y., Shaw, S. L., Zhao, Z., Yin, L., Zhang, T., & Lin, Y. (2016). Understanding spatiotemporal patterns of human convergence and divergence using mobile phone location data. *ISPRS International Journal of Geo-Information*, *5*(10). https://doi.org/10.3390/ijgi5100177

Yang, Y., Heppenstall, A., Turner, A., & Comber, A. (2019). A spatiotemporal and graph-based analysis of dockless bike sharing patterns to understand urban flows over the last mile. *Computers, Environment and Urban Systems*, *77*, 101361. https://doi.org/10.1016/j.compenvurbsys.2019.101361

Zaltz Austwick, M., O'Brien, O., Strano, E., & Viana, M. (2013). The Structure of Spatial Networks and Communities in Bicycle Sharing Systems. *PLoS ONE*, *8*(9), e74685. https://doi.org/10.1371/journal.pone.0074685

Zhang, Y., Brussel, M. J. G., Thomas, T., & van Maarseveen, M. F. A. M. (2018). Mining bike-sharing travel behavior data: An investigation into trip chains and transition activities. *Computers, Environment and Urban Systems*, *69*, 39–50. https://doi.org/https://doi.org/10.1016/j.compenvurbsys.2017.12.004

Zhang, Y., Thomas, T., Brussel, M., & van Maarseveen, M. (2017). Exploring the impact of built environment factors on the use of public bikes at bike stations:

Case study in Zhongshan, China. *Journal of Transport Geography*, *58*, 59–70. https://doi.org/10.1016/j.jtrangeo.2016.11.014

Zhang, Y., Lin, D., & Mi, Z. (2019). Electric fence planning for dockless bike-sharing services. *Journal of Cleaner Production*, *206*, 383–393. https://doi.org/10.1016/j.jclepro.2018.09.215

Zhao, P., & Li, S. (2018). Suburbanization, land use of TOD and lifestyle mobility in the suburbs: An examination of passengers' choice to live, shop and entertain in the metro station areas of Beijing. *Journal of Transport and Land Use*, *11*(1), 195–215. https://doi.org/10.5198/jtlu.2018.1099

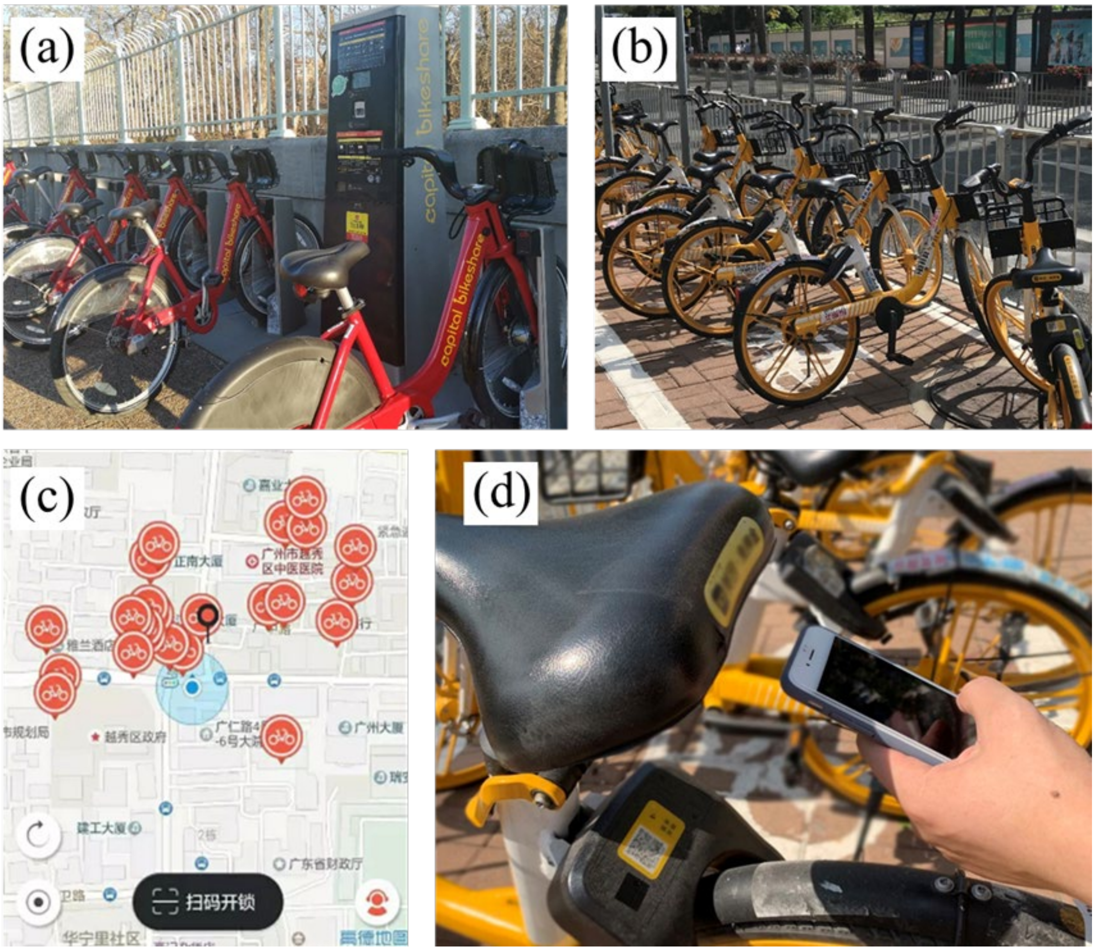


Figure 1. (a) An example of the bike-sharing system with docks (photographed by Xiaoyue Tan); (b) An example of the dockless bike-sharing system (photographed by Xiaolin Zhu); (c) Screenshot of a smartphone app for the dockless bike-sharing system that shows locations of available shared bikes; (d) Unlocking a shared bike by scanning the QR code for the dockless bike-sharing system (photographed by Xiaolin Zhu).

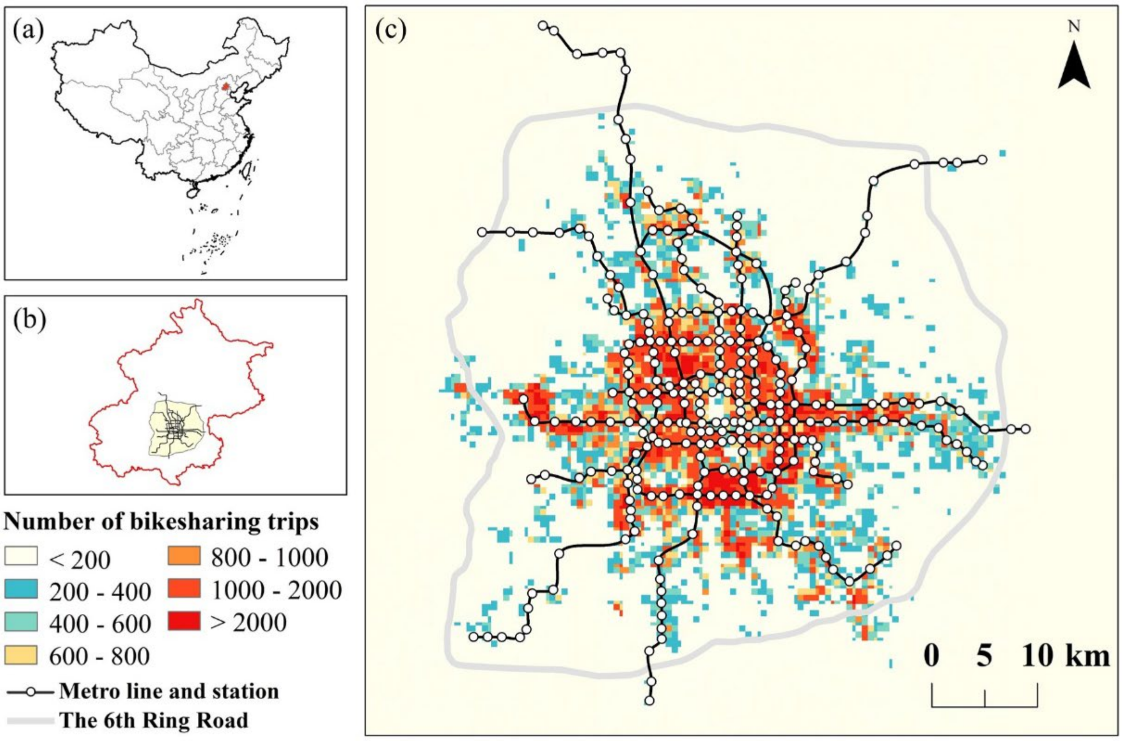


Figure 2. Location of study area in Beijing (b), the capital city of China (a). The public metro network and distribution of bike-sharing trips (sum of departures and arrivals in one week), mainly within the Sixth Ring Road in Beijing city (c).

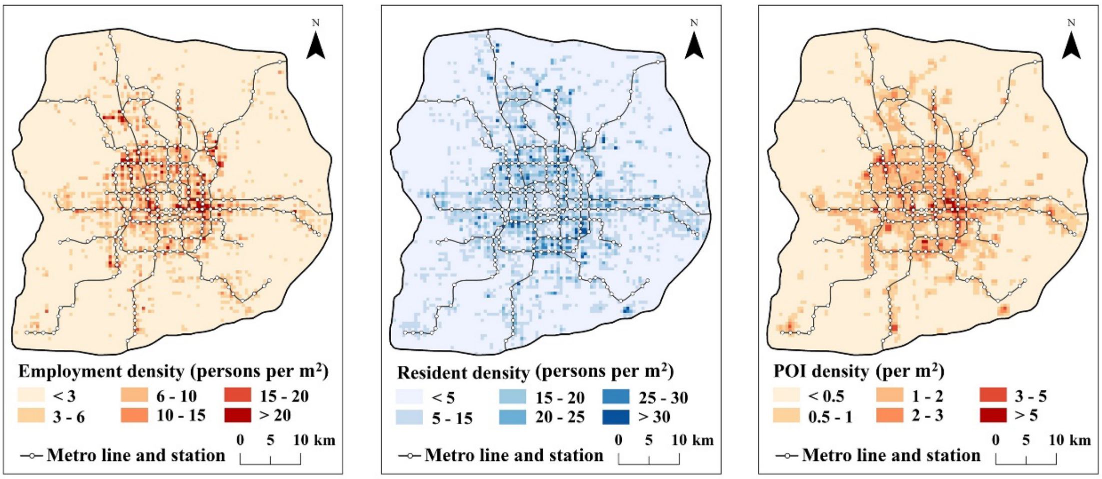


Figure 3. Density of people (a) working and (b) living within the Sixth Ring Road in Beijing city, (c) POI density.

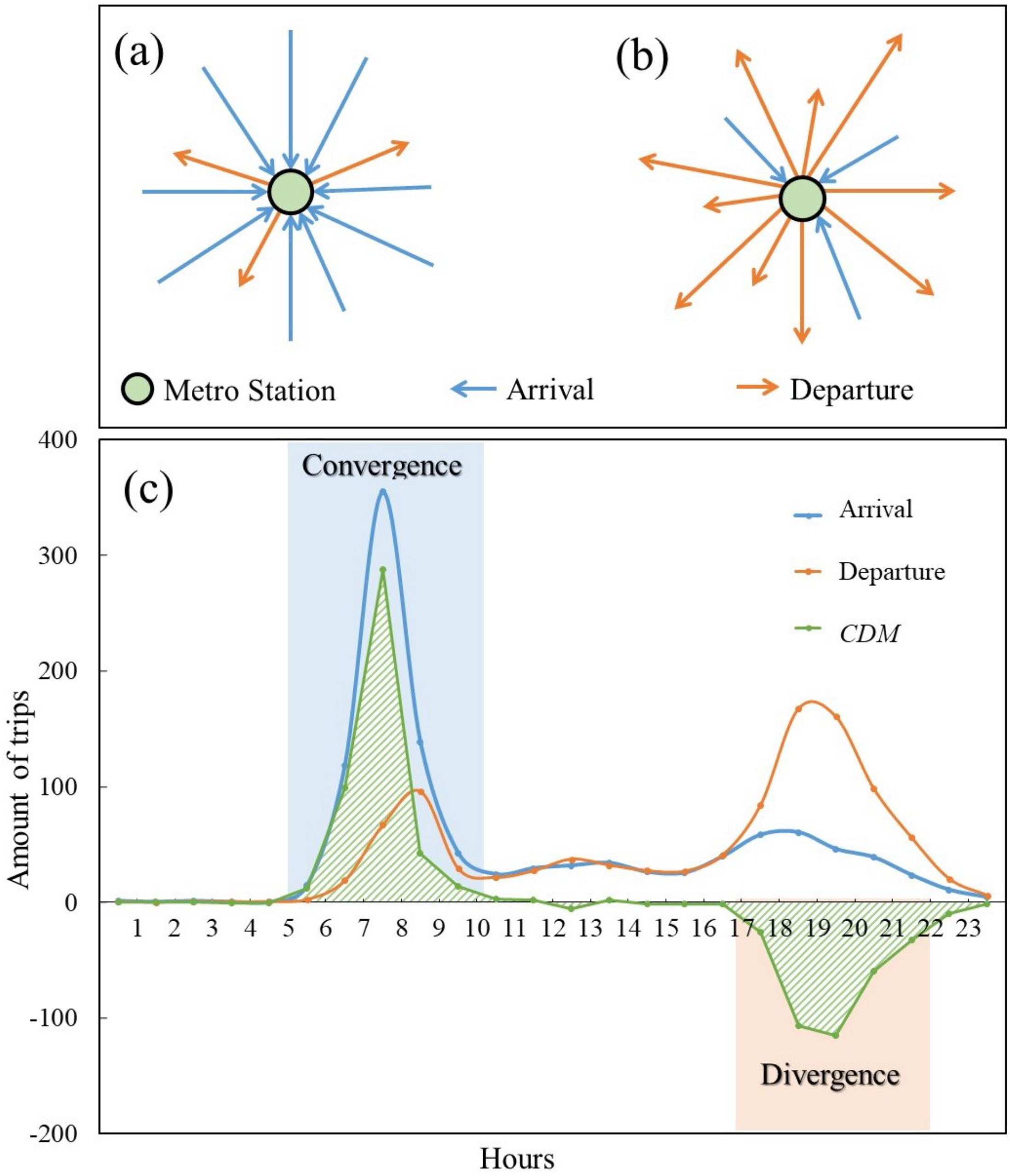


Figure 4. Schematic diagrams of convergence (a) and divergence (b) in a metro station, the changes of arrival flow, departure flow and corresponding convergence-divergence matrix (*CDM*) during a day (c).

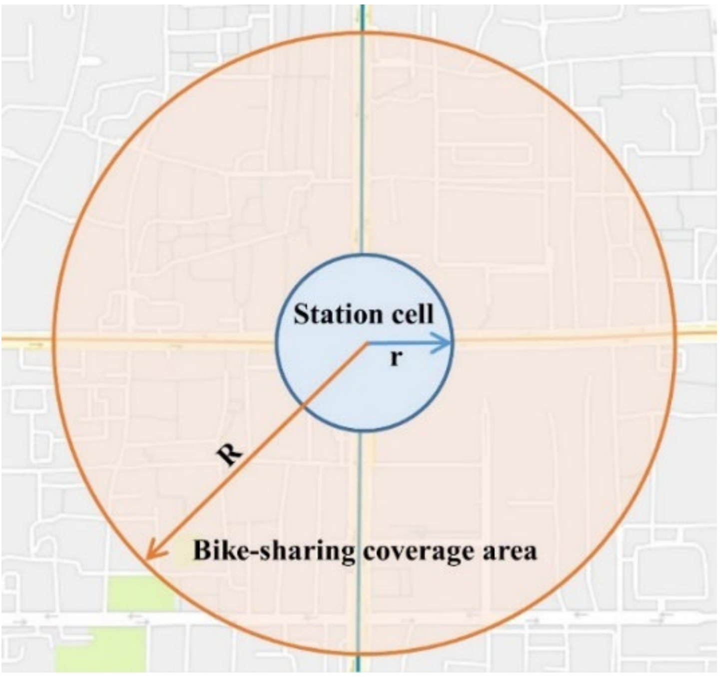


Figure 5. Schematic diagram of a station cell (blue) and corresponding bike-sharing coverage area (orange) along the metro lines (green and yellow).

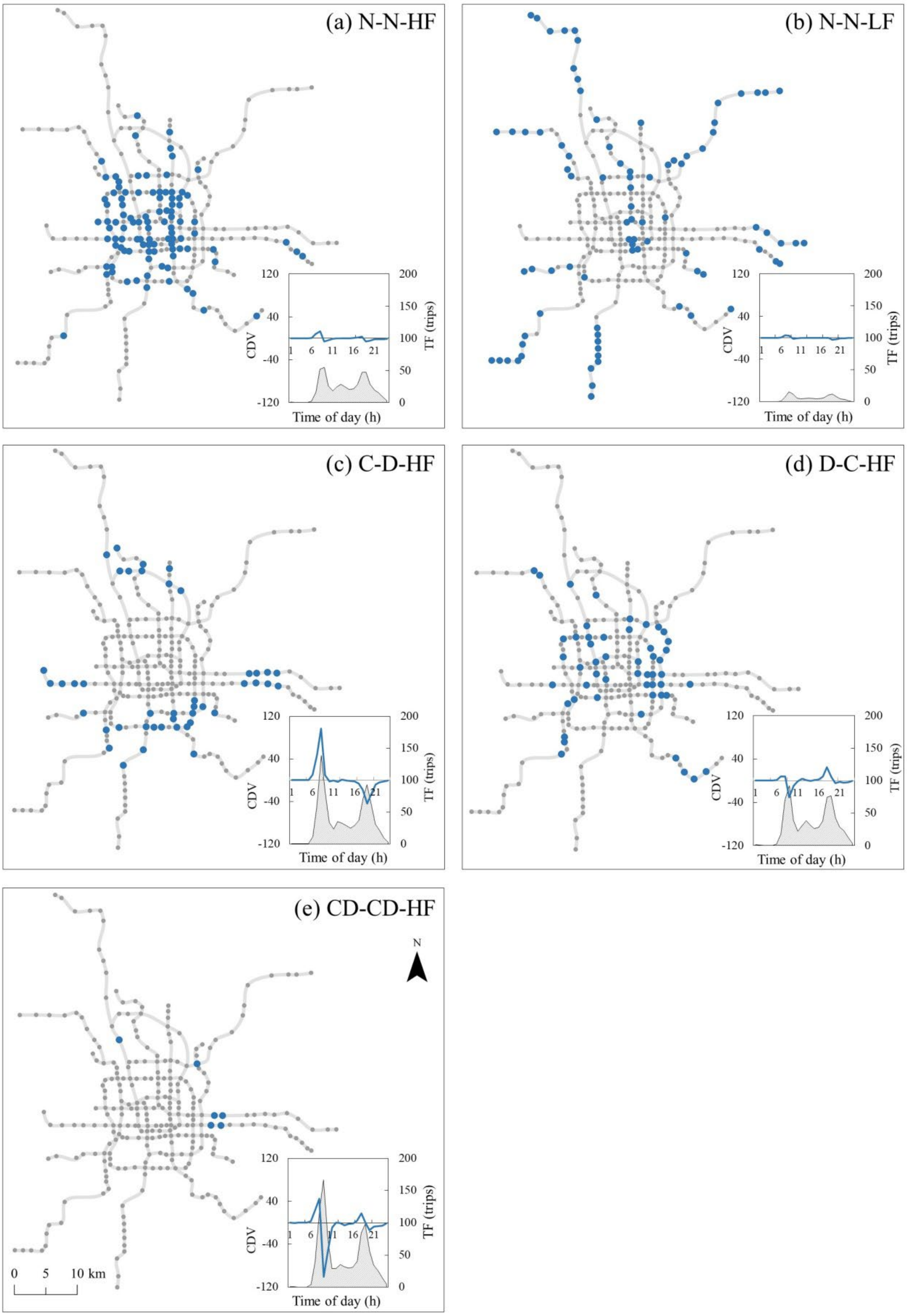


Figure 6. Metro station distribution of pattern N-N-HF (a), N-N-LF (b), C-D-HF (c), D-C-HF (d), CD-CD-HF (e) on weekdays, and corresponding hourly profile of *CDM* (blue) and *TF* (grey).

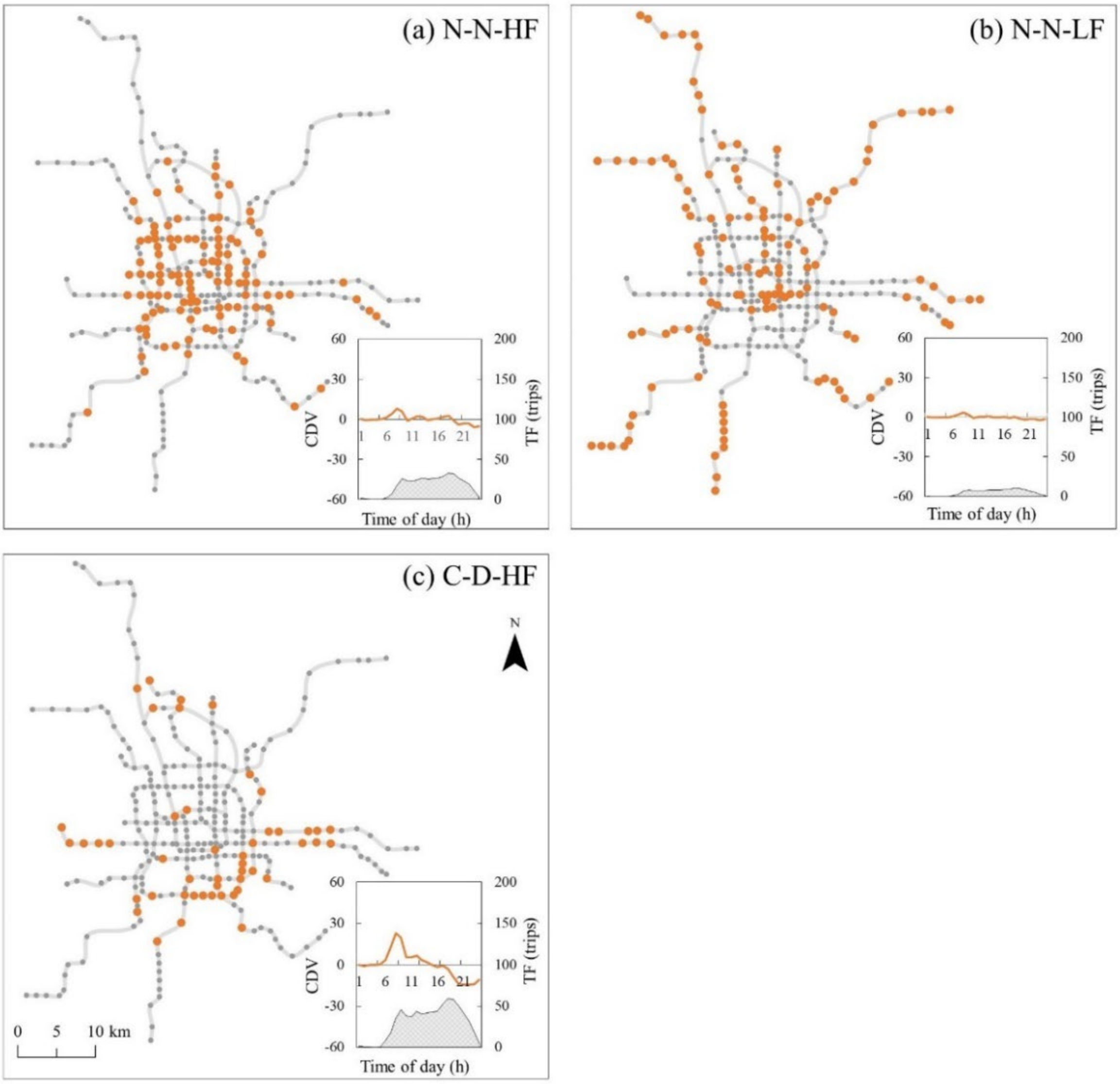


Figure 7. Metro station distribution of pattern N-N-HF (a), N-N-LF (b), C-D-HF (c) on weekends, and corresponding hourly profile of *CDM* (orange) and *TF* (grey)

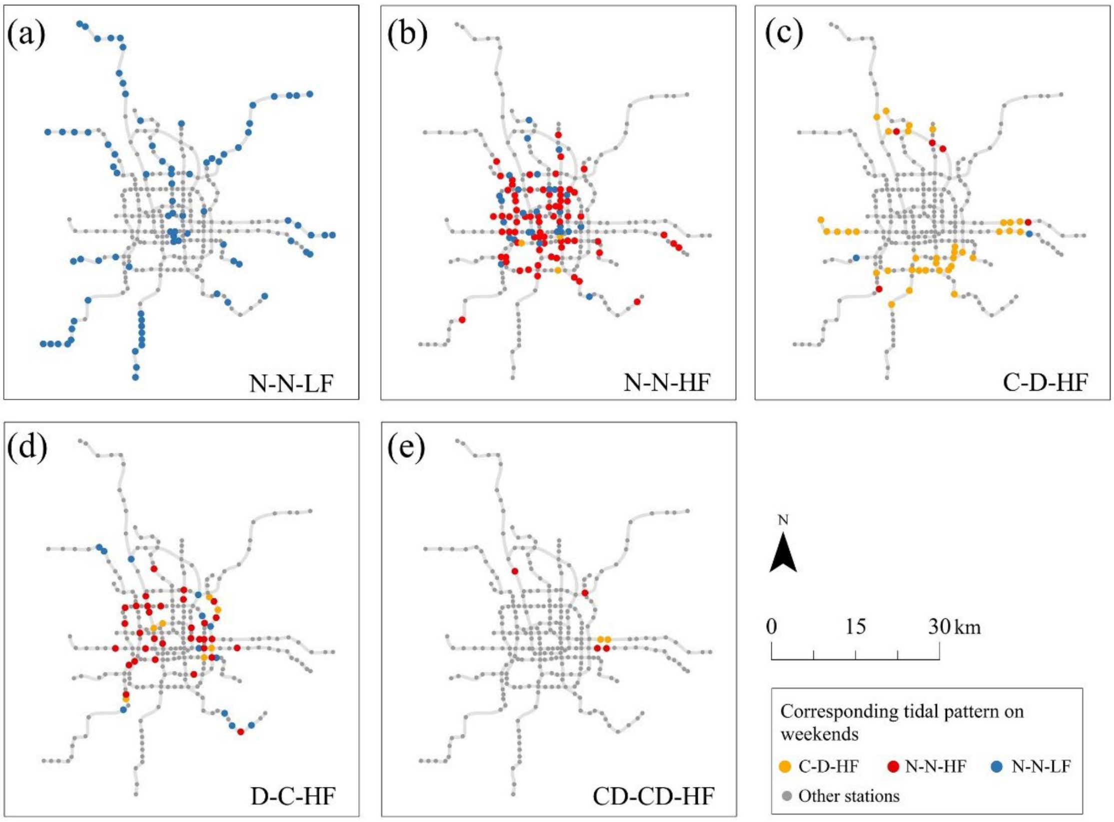


Figure 8. Corresponding tidal pattern on weekends for stations with pattern (a) N-N-LF, (b) N-N-HF, (c) C-D-HF, (d) D-C-HF and (e) CD-CD-HF on weekdays.

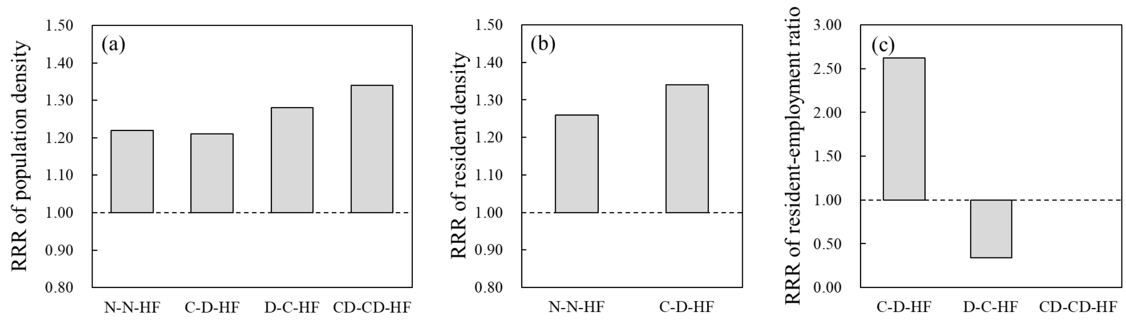


Figure 9. RRR values of (a) population density compared to N-N-LF on weekdays, (b) resident density compared to N-N-LF on weekends, (c) resident-employment ratio compared to N-N-HF on weekdays. Bars not shown in the histogram indicate that the impact is not significant.

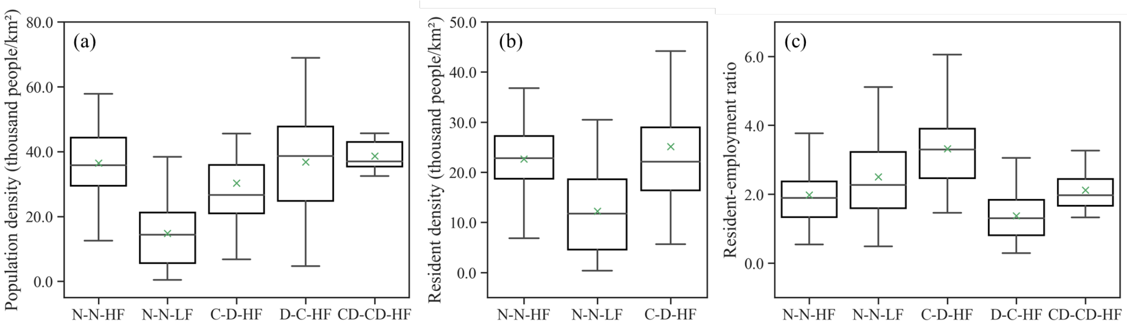


Figure 10. Statistics of influential factors in bike-sharing coverage area of each pattern: (a) population density based on weekday pattern, (b) resident density based on weekend pattern, (c) resident-employment ratio based on weekday pattern.

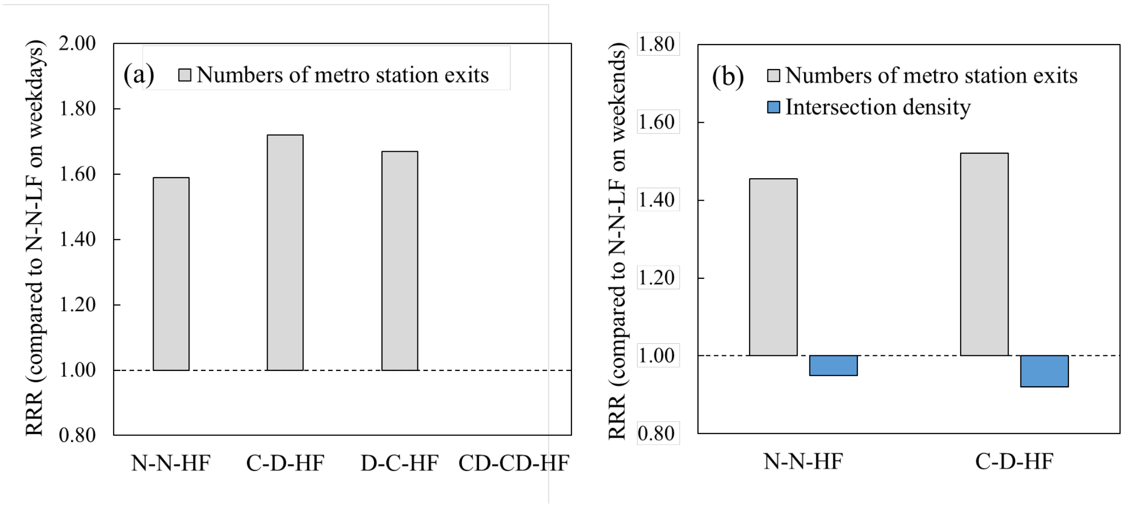


Figure 11. RRR of traffic condition factors compared to N-N-LF on (a) weekdays and (b) weekends, bars not shown in the histogram indicate that the impact is not significant.

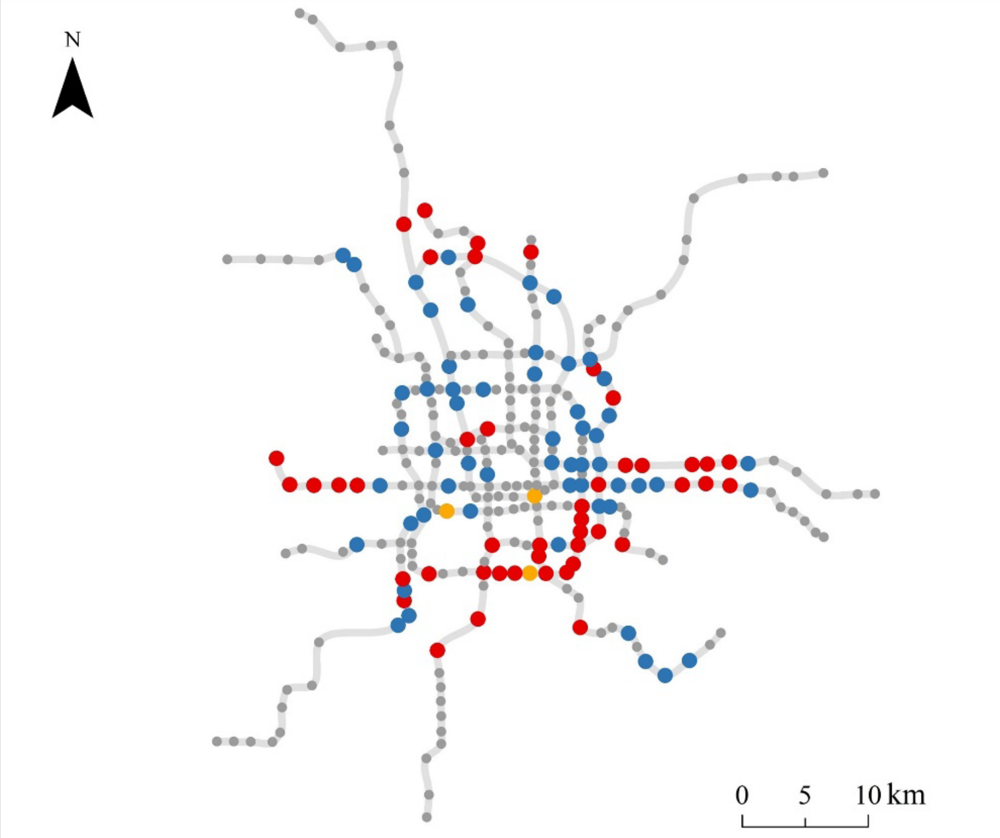


| Legend | Days that additional management is required on the peak hours | Patterns on weekdays | Patterns on weekends |
|---|---|---|---|
| ● | Weekday | C-D-HF/ D-C-HF/CD-CD-HF | N-N-LF/N-N-HF |
| ● | Weekend | N-N-LF/N-N-HF | C-D-HF |
| ● | Everyday | C-D-HF/ D-C-HF/CD-CD-HF | C-D-HF |
| ● | No additional management is required | N-N-LF/N-N-HF | N-N-LF/N-N-HF |

Figure 12. Arrangements for additional management and corresponding tidal traffic patterns on weekdays and weekends.

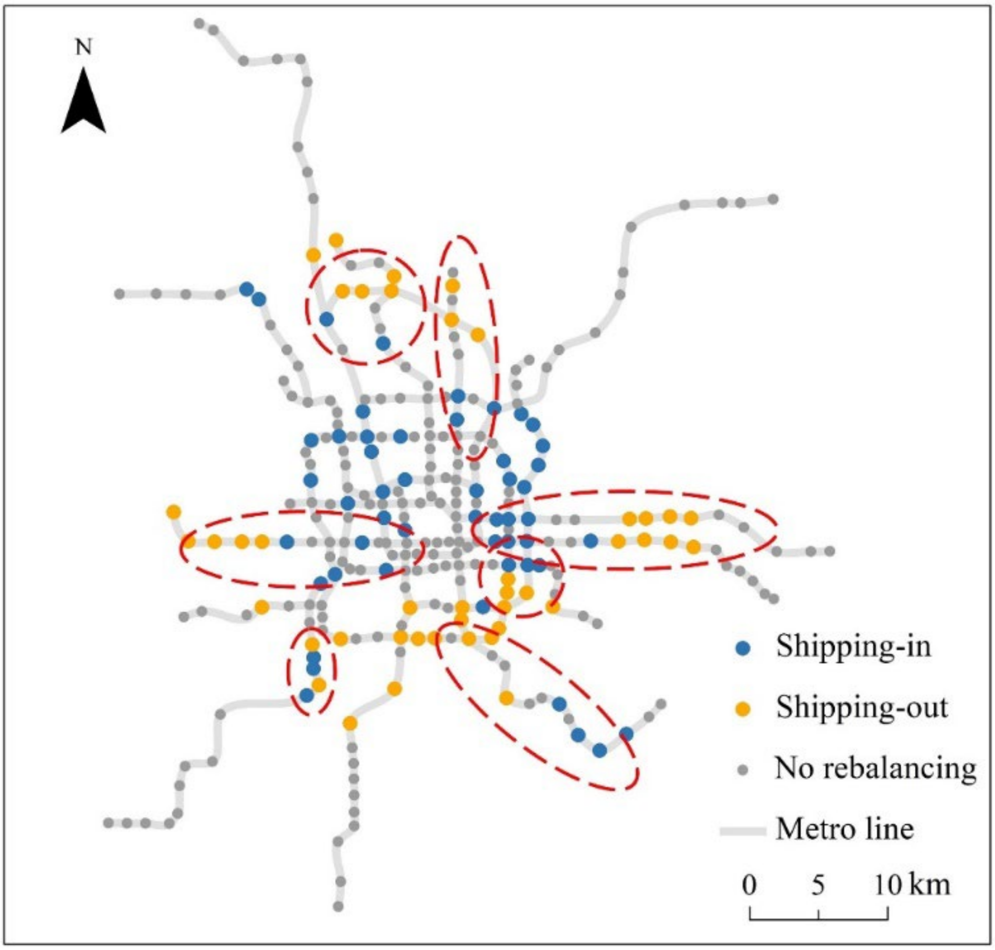


Figure 13. Rebalancing arrangement on weekday morning peaks, inside the red ellipse are some possible shipping-in and shipping-out pairs.

Table1. Descriptive statistics of the influential factors

| Factors | Mean | Std | Min | Max |
|---|---|---|---|---|
| ***Demographic*** | | | | |
| Population density (thousand people/km$^2$) | 29.19 | 16.20 | 0.43 | 91.81 |
| Resident density (thousand people/km$^2$) | 18.46 | 10.38 | 0.34 | 78.94 |
| Employment density (thousand people/km$^2$) | 10.72 | 8.18 | 0.09 | 44.49 |
| Resident-employment ratio | 2.23 | 1.22 | 0.29 | 7.55 |
| ***Traffic condition*** | | | | |
| Length of roads (km/km$^2$) | 5.56 | 2.20 | 0.62 | 10.48 |
| Intersection density (per km$^2$) | 11.69 | 6.68 | 0.00 | 34.06 |
| Bus stop density (per km$^2$) | 5.06 | 2.38 | 0.32 | 18.14 |
| Numbers of metro station exits | 4.13 | 1.82 | 1.00 | 12.00 |
| ***land use*** | | | | |
| Land use diversity (per km$^2$) | 1.77 | 0.22 | 0.52 | 2.07 |
| Land use density (per km$^2$) | 495.45 | 384.39 | 0.95 | 2663.30 |
| Restaurant density (per km$^2$) | 80.21 | 59.26 | 0.32 | 329.45 |
| Entertainment venue density (per km$^2$) | 3.52 | 2.82 | 0.00 | 14.96 |
| Pub/Bar density (per km$^2$) | 1.63 | 4.04 | 0.00 | 36.61 |
| Shop density (per km$^2$) | 125.89 | 169.94 | 0.38 | 2390.51 |
| Shopping mall (have=1, not=0) | 0.14 | 0.34 | 0.00 | 1.00 |
| Park density (per km$^2$) | 0.69 | 1.25 | 0.00 | 16.55 |
| Scenic spot density (per km$^2$) | 3.75 | 8.71 | 0.00 | 62.71 |
| Outdoor recreational place density (per km$^2$) | 0.77 | 0.74 | 0.00 | 4.14 |
| Elementary and secondary school density (per km$^2$) | 5.17 | 3.19 | 0.00 | 13.05 |
| University density (per km$^2$) | 8.68 | 15.30 | 0.00 | 114.59 |
| Government agency and institution density (per km$^2$) | 17.86 | 14.60 | 0.00 | 56.98 |

Table 2. Tidal traffic patterns for weekdays and weekends

| Patterns | N-N-HF | N-N-LF | C-D-HF | D-C-HF | CD-CD-HF |
|---|---|---|---|---|---|
| Weekdays | 34.86% | 29.93% | 15.14% | 17.96% | 2.11% |
| Weekends | 44.37% | 38.73% | 16.90% | - | - |

* All patterns were named as three segments according to their CDM and TF characteristics. The first two segments represent state of tidal traffic in morning and evening respectively and the third segment represents the level of total flow. N: No obvious convergence and divergence; C: Convergence; D: Divergence; CD: Convergence followed by divergence; HF: high total flow; LF: low total flow.

Table 3. The estimated results of MNLM on weekdays

| Explanatory variables | N-N-LF (base: N-N-HF) | | C-D-HF (base: N-N-HF) | | D-C-HF (base: N-N-HF) | | D-C-HF (base: C-D-HF) | | CD-CD-HF (base: N-N-HF) | | CD-CD-HF (base: C-D-HF) | | CD-CD-HF (base: D-C-HF) | |
|---|---|---|---|---|---|---|---|---|---|---|---|---|---|---|
| | RRR | z[1] | RRR | z | RRR | z | RRR | z | RRR | z | RRR | z | RRR | z |
| Population density | 0.82*** | -3.90 | 1.00 | -0.14 | 1.05 | 1.67 | 1.06 | 1.50 | 1.10* | 2.05 | 1.10* | 2.21 | 1.04* | 2.27 |
| Resident-employment ratio | 1.34 | 1.04 | 2.62*** | 3.45 | 0.34*** | -3.08 | 0.13*** | -5.13 | 0.44 | -1.6 | 0.17*** | -3.52 | 1.31 | 0.48 |
| Numbers of metro station exits | 0.63** | -2.55 | 1.08 | 0.64 | 1.05 | 0.46 | 0.97 | -0.22 | 0.81 | -0.49 | 0.75 | -0.67 | 0.77 | -0.59 |
| Land use diversity | 0.19 | -1.16 | 0.28 | -0.7 | 0.05* | -2.01 | 0.17 | -1.14 | 0.06 | -1.15 | 0.23 | -0.62 | 1.36 | 0.14 |
| Land use density | 1.00 | -1.36 | 1.00 | -0.91 | 1.00* | -2.24 | 1.00 | -0.73 | 0.99** | -2.87 | 0.99* | -1.97 | 1.00 | -1.54 |
| Restaurant density | 1.03*** | 2.86 | 1.02 | 1.58 | 1.02* | 2.03 | 1.00 | -0.12 | 1.04 | 1.86 | 1.02 | 1 | 1.02 | 1.09 |
| Elementary and secondary school density | 0.84 | -1.28 | 0.93 | -0.61 | 0.98 | -0.2 | 1.05 | 0.33 | 1.31 | 0.99 | 1.40 | 1.25 | 1.34 | 1.05 |
| University density | 0.99 | -0.19 | 0.99 | -0.72 | 0.98* | -2.12 | 0.99 | -0.50 | 0.75 | -1.44 | 0.76 | -1.38 | 0.77 | -1.33 |
| Government agency and institution density | 1.03 | 0.23 | 0.96 | -1.42 | 0.97 | -1.2 | 1.01 | 0.32 | 0.95 | -1.17 | 0.99 | -0.29 | 0.98 | -0.5 |
| (constant) | 1843.35** | 2.78 | 0.49 | -0.22 | 545.22* | 2.43 | 112.87** | 2.63 | 42.08 | 0.91 | 86.51 | 1.08 | 0.08 | -0.69 |

*** Significant at the 0.001 level.

** Significant at the 0.01 level.

* Significant at the 0.05 level.

[1] z is score for Z-Test of corresponding coefficient

Table 4. The estimated results of MNLM on weekends

| Explanatory variables | N-N-HF (base: N-N-LF) | | C-D-HF (base: N-N-LF) | | C-D-HF (base: N-N-HF) | |
|---|---|---|---|---|---|---|
| | RRR | z | RRR | z | RRR | z |
| Resident density | 1.26*** | 6.83 | 1.34*** | 6.43 | 1.06* | 2.11 |
| Intersection density | 0.95* | -1.98 | 0.92* | -1.98 | 0.97 | -0.95 |
| Numbers of metro station exits | 1.45*** | 3.70 | 1.52*** | 3.28 | 1.04 | 0.46 |
| Land use diversity | 0.66 | -0.38 | 0.18* | -2.30 | 0.27* | -2.32 |
| Land use density | 1.00 | 0.62 | 0.99* | -2.40 | 0.99** | -2.95 |
| Restaurant density | 0.99 | -1.82 | 1.02 | 1.70 | 1.03** | 2.86 |
| Pub/Bar density | 1.05* | 2.09 | 0.82 | -1.80 | 0.78* | -2.22 |
| Shopping mall | 1.99* | 2.15 | 3.89* | 2.26 | 1.96 | 1.39 |
| (constant) | 0.02* | -2.13 | 0.05 | -1.43 | 2.38 | 0.35 |

*** Significant at the 0.001 level.

** Significant at the 0.01 level.

* Significant at the 0.05 level.